

INVESTIGATION OF RESIDUAL STRESSES IN AS-WELDED AND TIG-DRESSED SPECIMENS SUBJECTED TO STATIC/SPECTRUM LOADING

L. Lopez Martinez*, R. Lin**, D.Wang** and A.F. Blom***

This paper deals with measurements of residual stresses by neutron diffraction in several conditions. Both the as welded and the TIG-dressed conditions are studied. The relaxation of weld-induced residual stresses is investigated by removing the test specimens and performing measurements during spectrum fatigue loading as function of number of load cycles. Neutron diffraction results are also compared to ultrasonic 3D-measurements as well as to x-ray diffraction results on the surface.

INTRODUCTION

Together with stress concentrations and weld defects, residual stress fields are one of the determinant parameters controlling the fatigue strength of welded joints (1). In normal fatigue design the level of residual stresses is unknown and therefore it is assumed that this level is in the same order as the yield strength of the filler metal. This fact leads to the assumption that the entire stress range, irrespective of stress ratio, produces fatigue damage. Residual stress distributions are also influenced by other parameters such as metallurgical properties, the welding technique used, and the heat input, Legatt (2).

The change of residual stress distribution through thickness by relaxation is a main factor influencing fatigue crack growth in welded components. For current fracture mechanics modeling an understanding of relaxations and redistribution of residual stresses is of vital interest.

* SSAB Oxelösund AB, S-613 80 Oxelösund, SWEDEN

** Studvik Neutron Research Laboratory, S-611 82 Nyköping, SWEDEN

*** FFA, P.O. Box 11021, S-161 11 Bromma, SWEDEN

The present paper deals with residual stresses in welded fatigue test specimens. It is a part of a current Nordic program which aims at improving fatigue design assessment for high-strength steels. By neutron diffraction and X-ray diffraction, residual stress distributions in as-welded and TIG-dressed specimens were non-destructively measured. In addition, the effects of both static and spectrum fatigue loading were evaluated. Results are also compared to ultrasonic 3D-measurements.

MATERIALS AND FATIGUE TESTING

The material used in this investigation has the strength properties and chemical composition shown in Table 1. For more details, see reference (1).

TABLE 1- Chemical compositions and tensile properties of steel

Chemical composition (wt%)							Yield strength (MPa)	Tensile strength (MPa)	Nominal strength (MPa)
C	Si	Mn	P	S	Al	Nb			
0.09	0.21	1,63	0.11	0.02	0.03	0.024	615	757	590

Spectrum fatigue testing and static loading were performed on specimens with a longitudinal fillet welded attachment also used in other investigations (3), see Fig. 1. The spectrum type is the same as used earlier, SP2 (R=0-0.77), a straight-line range-pair counted spectrum with I=1.0. The maximum applied stress, σ_{max} , in the test spectrum was chosen to be the same as the selected static load, i.e. 250 MPa. This value was chosen to produce plastic deformation in the vicinity of the weld root. The fatigue tests were carried out at FFA in Stockholm.

The welding procedure was MAG with 1.6 mm electrode, current of 185 Amp (DC), voltage = 23,5 Volt and heat input approximately 1.5 KJ/mm with consumable PZ 6130 (Mison 25), performed without pre-heating. The welds on the sides of the attachments as well as at the corners have been produced in an alternating diagonal sequence in order to limit the interpass temperature (<250° C), as well as specimen distortion.

Since all specimens have been produced in the same way, the residual stress fields should have very similar pattern and, therefore, should be representative also for the rest of the specimens tested within the Nordic programme for the same steel.

RESIDUAL STRESS MEASUREMENTS

Neutron diffraction measurements of residual stress were carried out with the REST diffractometer at the R2 Reactor in Studsvik, Sweden. The technique uses atomic interplanar spacing as internal strain gauge and measures changes in the interplanar spacing due to stresses. Strains are then calculated by the following equation.

$$\varepsilon_{hkl} = \frac{d_{hkl} - d_{hkl}^{\circ}}{d_{hkl}^{\circ}} \quad (1)$$

where d_{hkl} and d_{hkl}° are the stressed and the stress-free interplanar spacing, respectively.

If the three principle strain components, ε_i , are obtained, residual stresses can be derived using Hooke's law:

$$\sigma_i = \frac{E_{hkl}}{1+\nu} \left[\varepsilon_i + \frac{\nu}{1-2\nu} \sum \varepsilon_j \right] \quad (2)$$

Where σ_i , $i = 1$ to 3 , are the three principle stress components; E_{hkl} and ν are the Young's modulus and Poisson's ratio, for the corresponding crystallographic orientation, respectively. Only longitudinal stresses are presented in this paper as they play a dominant role in fatigue life for the component.

Residual stress distributions were measured in the as-welded and TIG-dressed conditions. The specimens were then subjected to fatigue spectrum loading and residual stress measurements were performed after 500.000 and 2.000.000 cycles. Residual stress distributions were also measured in two other specimens before and after static loading up to 250 MPa.

The locations for stress measurements are shown in Figs 2 and 3. At these locations both the level of residual stresses and subsequent relaxation were expected to be pronounced. The first cross section, indicated by "A", was chosen to be near the weld toe and was 13 mm from the end of the attachment. Fatigue failure was mostly confined to this cross section for the as-welded specimens. The second cross section, named "B", was prone to fatigue failure for the TIG-dressed specimens. The last cross section "C" was at the mid-width of the plate. Strains parallel to the specimen's natural co-ordinates, i.e. the longitudinal transverse and normal directions, were obtained and were assumed to be the principle directions. Residual stresses were therefore calculated from the measured strains using Eq. (2), with Young's modulus $E_{hkl} = 225$ GPa and a Poisson's ratio $\nu = 0.285$. Both were calculated from Fe single crystal elastic constants by the Kröner model.

The specimen geometry indicates a symmetrical stress field about the mid-plane and about the mid-width, which was confirmed by preliminary neutron diffraction measurements and by X-ray diffraction measurements at the surface. Therefore, only

through half-thickness stress distributions were mapped. The incident slit, which defines the size of the incoming neutron beam, was 2 mm wide and 2 mm high. With a receiving slit of 2 mm width, the spatial resolution in all the three directions can be approximated about 2 mm.

The stress-free lattice spacing was obtained by measuring on small coupons cut from different locations in an as-welded plate and an as-welded and TIG-dressed plate. They were crosschecked by measuring, in each specimen, a location, which was far away from the weld. Standard deviations in strains were typically smaller than $\pm 1 \times 10^{-4}$, calculated from uncertainties in peak fitting. The resulting errors in residual stresses are less than ± 25 MPa. These errors are caused from uncertainties in peak fitting, gage volume and metallurgical changes in the heat-affected zone.

RESULTS AND DISCUSSIONS

Residual stresses due to welding

Tensile residual stresses were observed in both A and B sections in the as-welded specimen, see Fig. 4. The maximum stress, close to the yield strength of the material, was found in close proximity to the surface at the weld toe. It decreases with increasing distance from the weld toe and from the surface.

Influence of TIG-dressing on distribution of welding residual stresses

The application of TIG-dressing on the weld toe has a strong effect on the local stress distribution. A comparison of Fig. 4a to Fig. 5a, shows clearly how the tensile stress component was increased from 556 to 699 MPa. As result, much lower tensile stress was found near the surface. This is consistent with X-ray diffraction measurements at the surface where tensile stress was decreased from 360 to 256 MPa by the TIG-dressing operation. These results confirm the hypotheses that TIG-dressing increases fatigue resistance not only by improving weld geometry, i.e. reducing the stress concentration factor, but also by reducing the tensile residual stress near the surface.

At the TIG-dressed edge, the tensile stress was increased near the surface while the compressive stress near the specimen edge became larger; compare Fig. 5b to Fig. 4b

Relaxation by static load

As the weld toe, where max. stress concentration is found, is already at the yield point of the weld metal, σ_{ywm} , static tensile loading, σ_{max} , would cause local plastic deformation and the stresses in the weld remains at yield level, σ_{ywm} , while the surrounding stress field changes to accommodate the applied load. When the applied load is removed, the residual stress distribution was altered to the level shown in Fig. 6 for the as-welded condition and in Fig. 7 for the TIG-dressed condition. The maximum residual stress was decreased by 200 MPa for the as-welded specimen and 130 MPa for the TIG-dressed specimen.

Relaxation under variable amplitude fatigue testing

It follows, therefore, that if σ_{\max} is repeatedly applied, i.e. fatigue loading ranging from zero to σ_{\max} , the actual stress will cycle between a minimum value of $\sigma_{\text{ywm}} - \sigma_{\max}$ and a maximum value of σ_{\max} i.e. at a range equal to the nominal range applied, but with a mean value different from that calculated from $\sigma_{\max} / 2$. In the case of variable amplitude fatigue testing we are not cycling from 0 to σ_{\max} every cycle so the situation changes drastically. Only a few times the σ_{\max} is applied at every block of 5×10^5 cycles so the change of residual stresses in the surrounding field to accommodate the applied load is mostly influenced by the level of σ_{\max} on each block. In Fig. 8 we present the results for relaxation studies in the as-welded condition and in Fig. 9 for TIG-dressed conditions. The relaxation occurs, major part of it, early during the fatigue load sequence. For the following fatigue load intervals we can see that relaxation occurs as redistribution of the residual stress field.

Correlation with X-ray diffraction measurements

Residual stresses at the surface of the as welded and the TIG-dresses specimens were also measured by X-ray diffraction. The results are presented in Fig. 10 and 11, jointly with measurements done by neutron diffraction at 1 mm depth. It should be noted that the X-ray measurements reveal stresses in a very thin surface layer while the neutron diffraction measurements show average stress in a 2^3 mm^3 gauge volume, thus they are not directly comparable.

Correlation with acoustic diffraction measurements

The results from neutron diffraction measurements at A-location for the longitudinal stress at mid-thickness can only be correlated to measurements carried out by acoustic diffraction, ultrasonic waves. Such measurements are presented in detail by Kudryavtsev et al (4). However, these measurements were performed on DOMEX 350 steel, so a direct comparison is not possible. Yet, it is interesting to note that both these 3D techniques present similar trends in the shape of the mid-plane residual stress distribution see Figs. 12 and 13. More work is needed to fully understand the total complex 3D residual stress fields.

CONCLUSIONS

Large longitudinal tensile stresses in the order of yield levels were found at the surface close to the weld toe. TIG-dressing was shown to shift the tensile stress peak into the depth of the specimens.

Relaxation studies haven shown that a static load applied did relax residual stresses as expected. The applied variable amplitude loading did show the same degree of relaxation as the static load case. This relaxation occurs early during the fatigue loading and is correlated to the occurrence of maximum load in the spectrum.

Good agreement in residual stress shape was been found for the measurement methods studied. However, the magnitudes were found to be different for different methods. The exact reason for this is not yet fully understood, but is probably due to several factors.

It is interesting to notice that the different results from the three methods were obtained by very well known laboratories (Studsvik Neutron Research Laboratory for neutron diffraction, Linköping Institute of Technology for X-ray diffraction, and Paton Electric Welding Institute, Kiev, for ultrasonic measurements). Yet, the mentioned difference still exists. Thus, any data interpretation should be somewhat cautions until a more complete understanding is obtained.

ACKNOWLEDGEMENTS

This work was financially supported by NI (Nordic Industrial Foundation), NUTEK (Swedish National Board for Industrial and Technical Development), SSAB, and FFA. The authors are indebted to Mr. Bengt Wahlstenius (FFA) for performing the fatigue tests and Mr. Tommy Kinden (SSAB Oxelösund AB) for performing welding and TIG-dressing.

REFERENCES

- (1) Lopez Martinez, L. and Blom A.F. "Influence of life improvement techniques on different steel grades under fatigue loading", Fatigue Design 95 Proceedings, Espoo, Finland, Edited by G. Marquis, 1995.
- (2) Legatt, R. "Welding Residual Stresses", ICRS 5, June 16-18, 1997, Linköping, Sweden.
- (3) Bogren, J., Lopez Martinez, L. « Spectrum fatigue testing and residual stress measurements on non-load carrying fillet welded test specimens" Proceedings of the Nordic Conference on Fatigue. Edited by A.F. Blom, EMAS Publishers, West Midlands, England, 1993.
- (4) Kudryavtsev, Y. et al "Measurement of residual stresses in welded specimens containing non-load-carrying fillet welds in as-welded condition and after TIG-dressing", Test report 201/3, Kiev 1996.

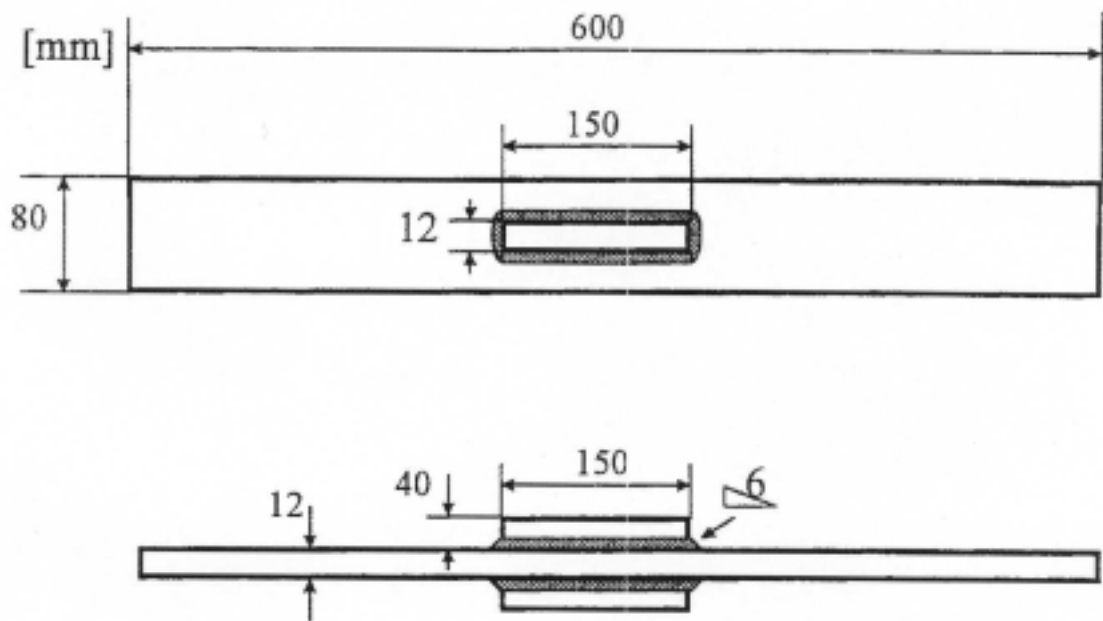


Figure 1 Fatigue test specimen

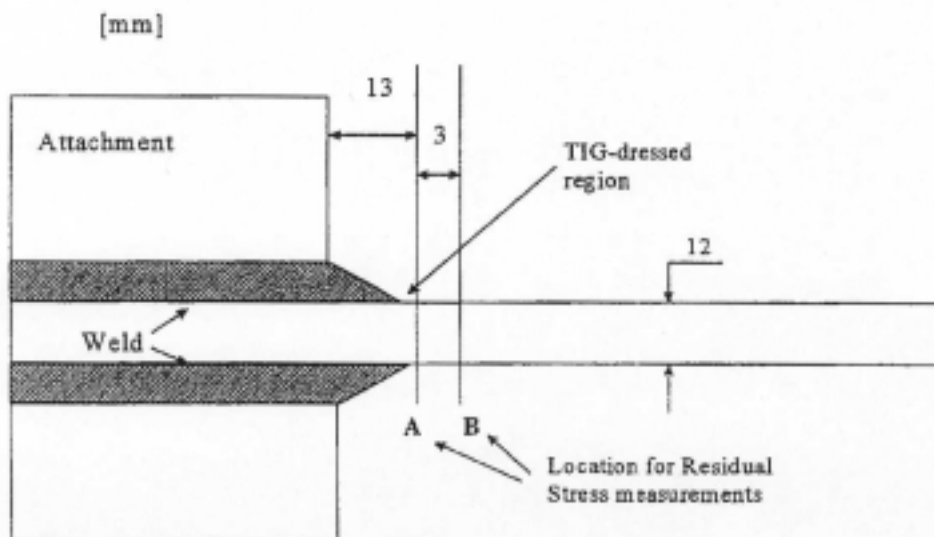


Figure 2 Specimen mid-section showing location for residual stress measurements

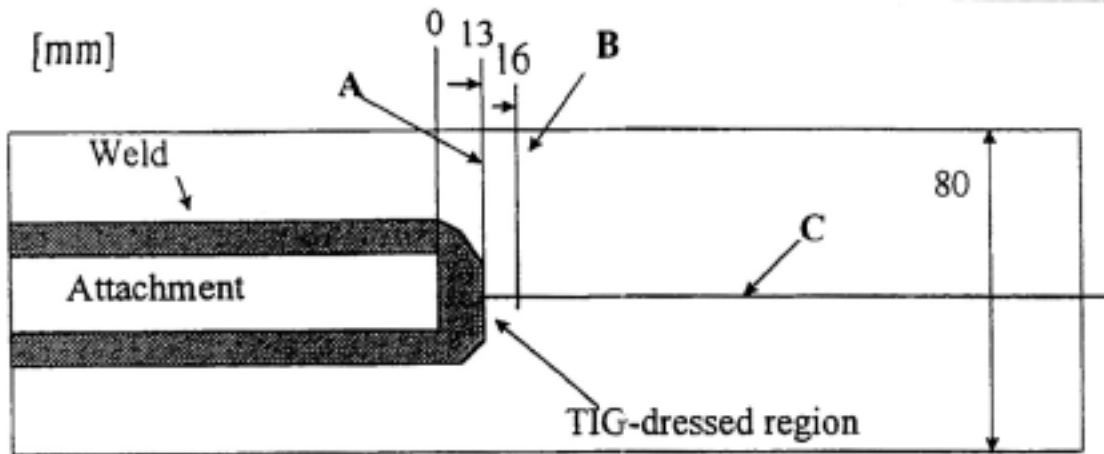


Figure 3 Upper view showing fatigue test specimen with locations for residual stress measurements

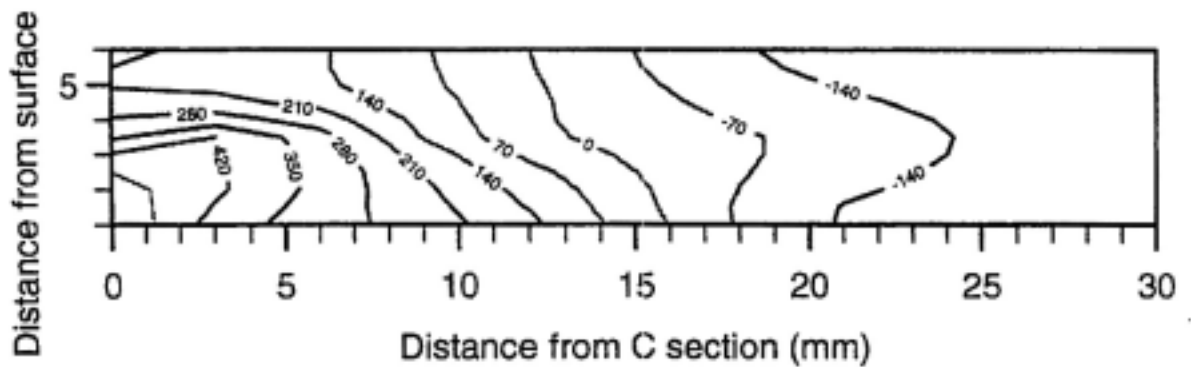


Figure 4a Longitudinal residual stress distribution in A-section of as-welded specimen

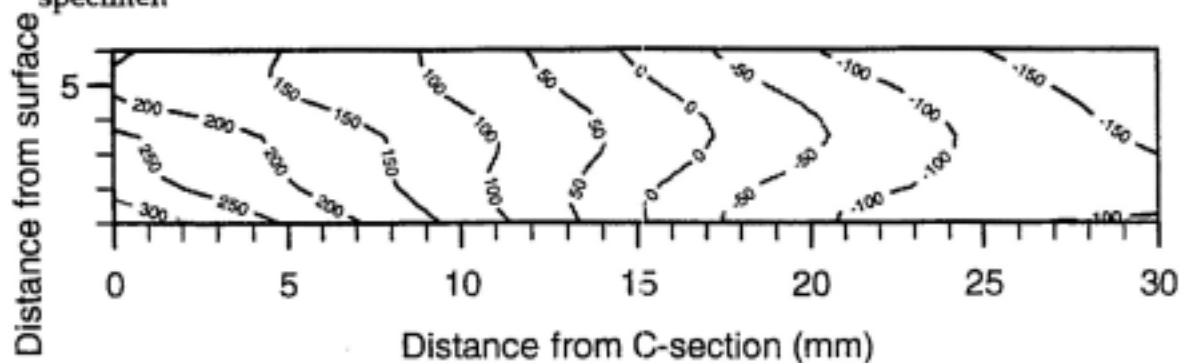


Figure 4b Longitudinal residual stress distribution in B-section of as-welded specimen

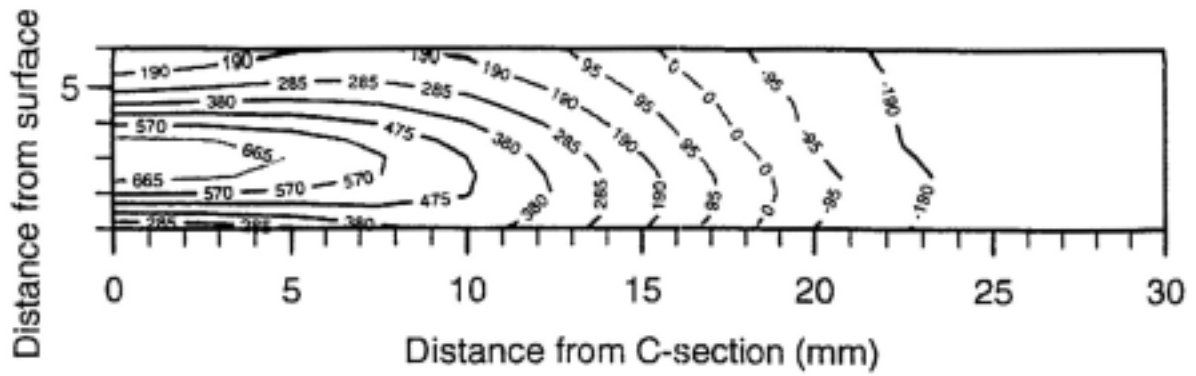


Figure 5a Longitudinal residual stress distribution in A-section of TIG-dressed specimen

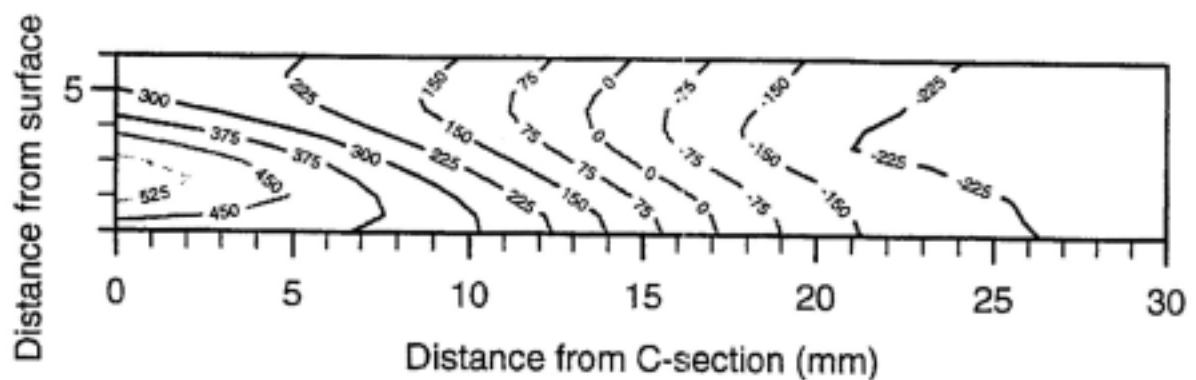


Figure 5b Longitudinal residual stress distribution in B-section of TIG-dressed specimen

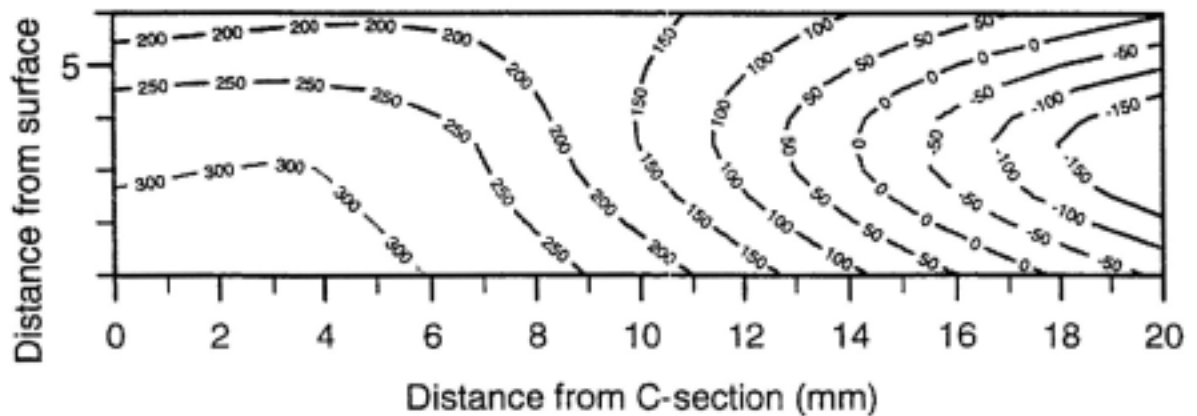


Figure 6 Longitudinal residual stress distribution in A-section of as-welded specimen following static loading

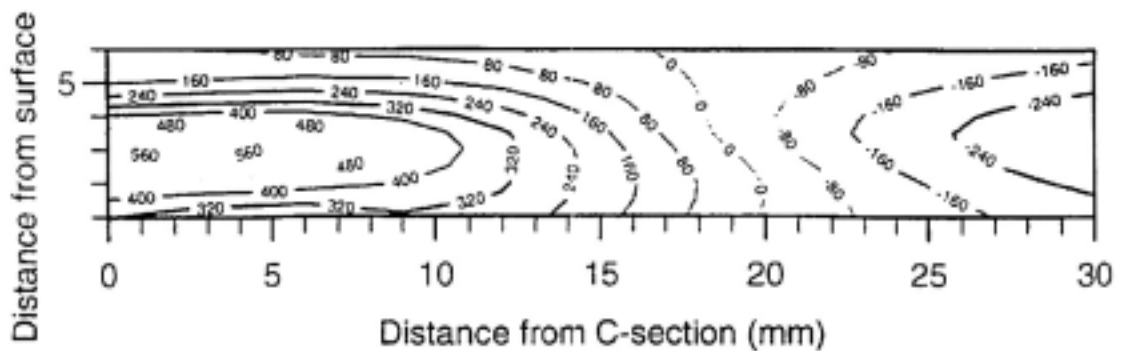


Figure 7 Longitudinal residual stress distribution in A-section of TIG-dressed specimen following static loading

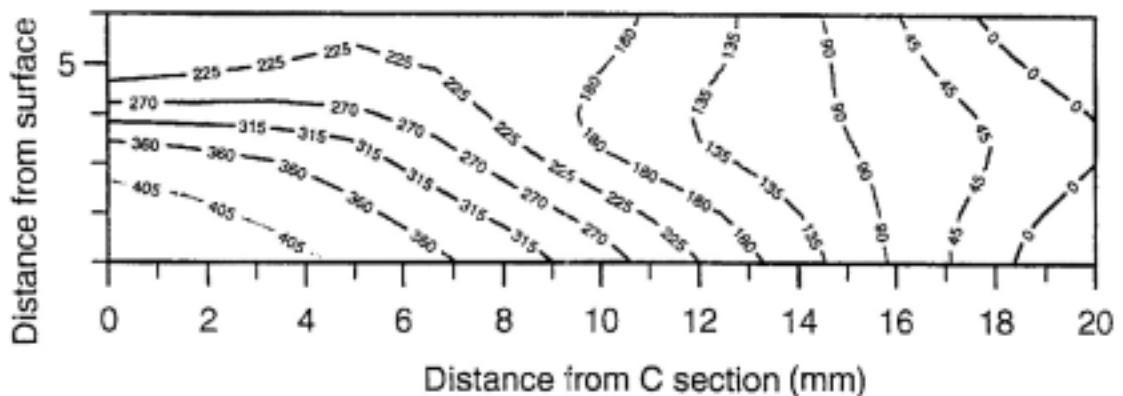


Figure 8a Longitudinal residual stress distribution in A-section of as-welded specimen after 500,000 cycles of spectrum loading

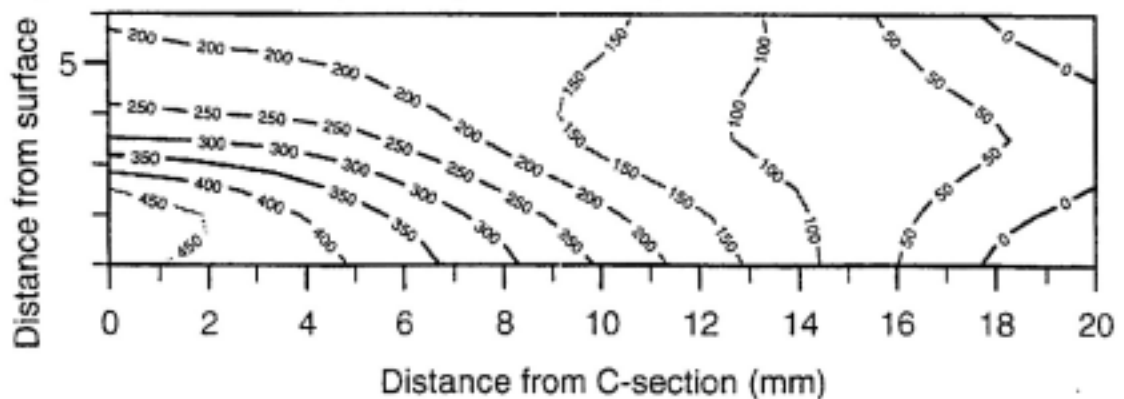


Figure 8b Longitudinal residual stress distribution in A-section of as-welded specimen after 2 million cycles of spectrum loading

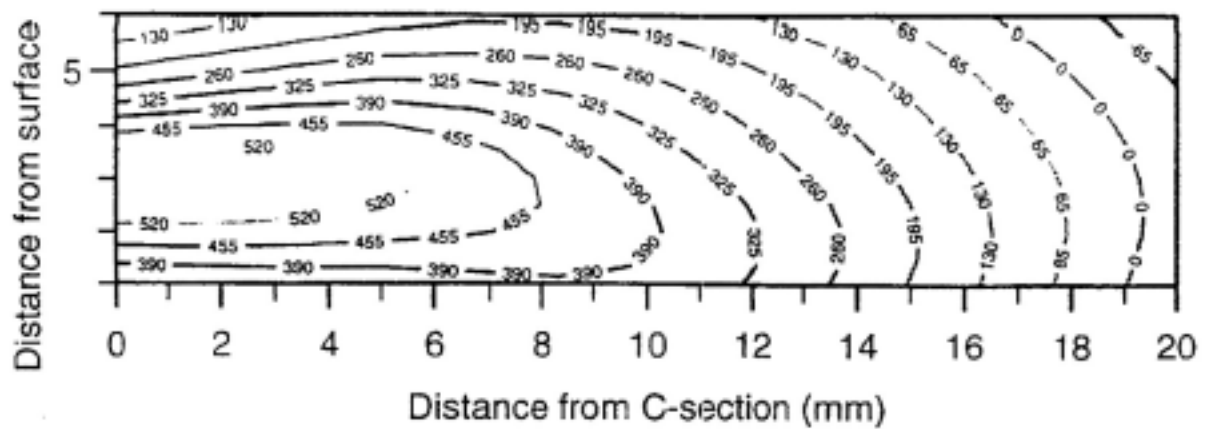


Figure 9a Longitudinal residual stress distribution in A-section of TIG-dressed specimen after 500,000 cycles of spectrum loading

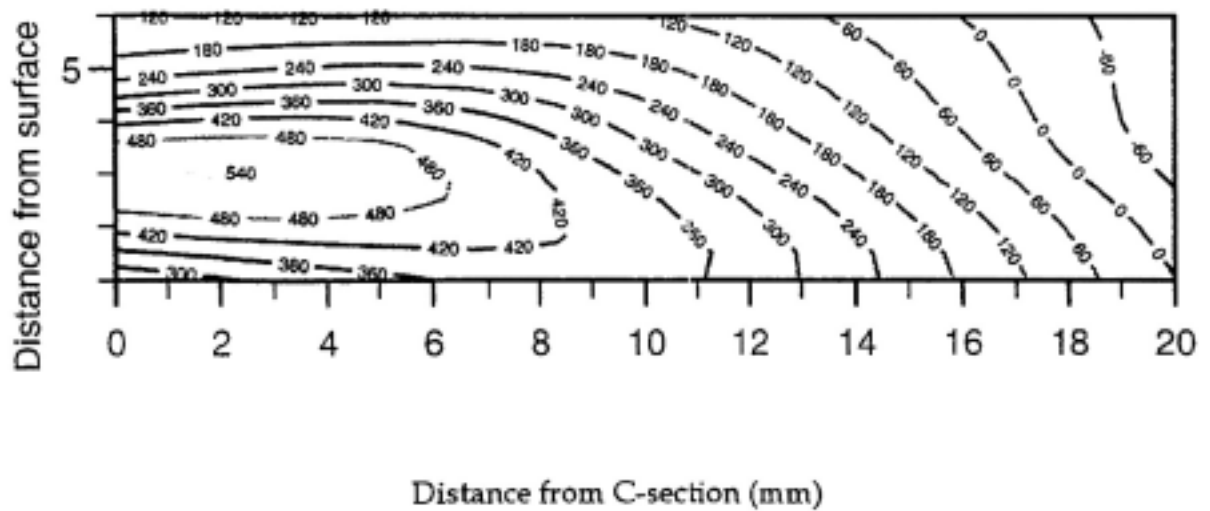


Figure 9b Longitudinal residual stress distribution in A-section of TIG-dressed specimen after 2 million cycles of spectrum loading

Longitudinal residual stresses at surface in the
As-welded condition

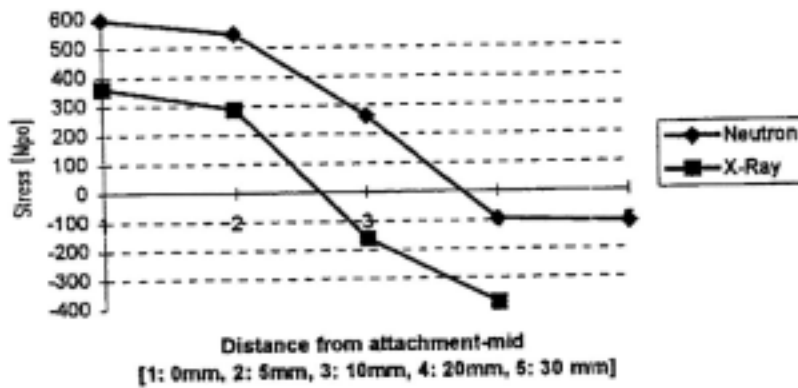


Figure 10 Measurement results at near surface: Neutron diffraction at 1 mm depth and χ -Ray diffraction at 10 μ depth .

Longitudinal residual stresses at surface for
TIG-dressed specimens

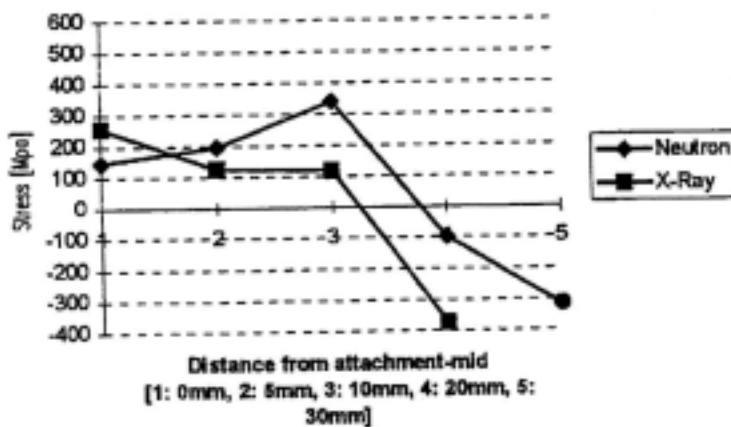


Figure 11 Measurement results for the TIG-dressed condition

Longitudinal residual stresses at mid-thickness
in the As-welded condition

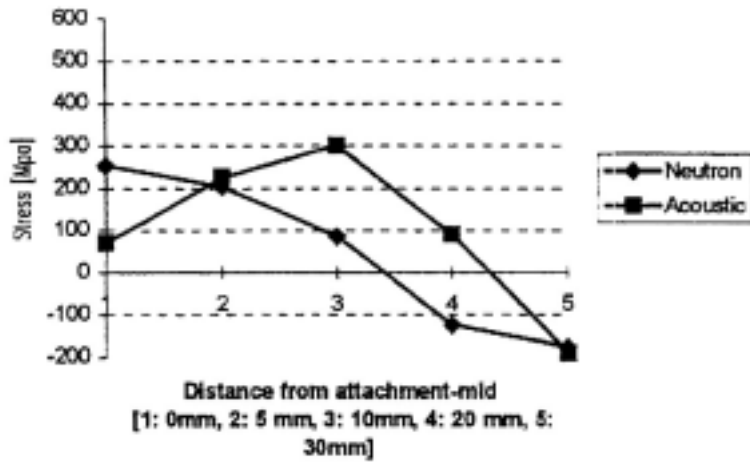


Figure 12 Measurements at mid-thickness: as-welded condition. Neutron dif-
fraction data for 590 steel, ultrasonic data for 350 steel

Longitudinal residual stresses at mid-thickness
in the TIG-dressed condition

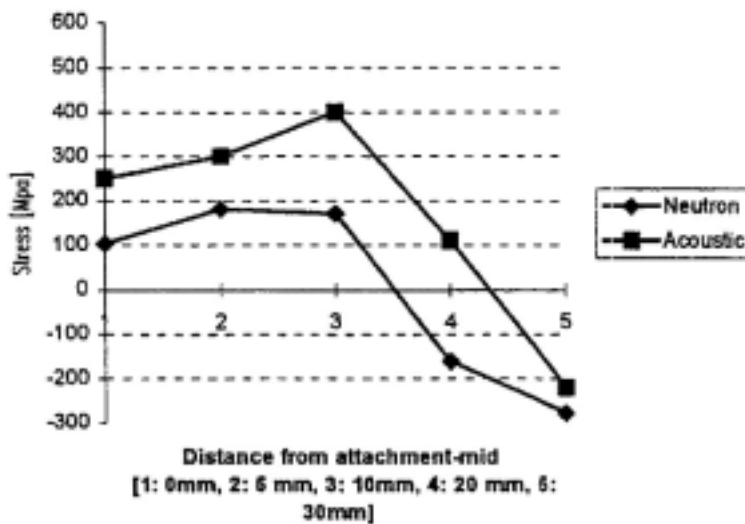


Figure 13 Measurements at mid-thickness: TIG-dressed condition. Neutron dif-
fraction data for 590 steel, ultrasonic data for 350 steel